XIX Encontro Nacional de Tecnologia do Ambiente Construído
ENTAC 2022

Ambiente Construído: Resiliente e Sustentável
Canela, Brasil, 9 a 11 novembro de 2022

Thermal calibration of an existing institutional building

Calibração térmica para uma edificação institucional existente

Caio de Carvalho Lucarelli

Universidade Federal de Viçosa | Viçosa | Brasil | lucarelli.caio@outlook.com

Matheus Menezes Oliveira

Universidade Federal de Viçosa | Viçosa | Brasil | matheus.meneses@gmail.com

Joyce Correna Carlo

Universidade Federal de Viçosa | Viçosa | Brasil | joyce.carlo@ufv.br

Abstract

Building performance simulation (BPS) exhibits an interplay of various physical parameters, only portraying limited building fundamental characteristics. Therefore, BPS calibration can increase simulation accuracy and better depict the physical space. We aimed to calibrate/validate an institutional building model in Viçosa-MG, testing parallel and serial uncertainty procedures. We conducted a manual/statistic hygrothermal calibration using surveyed indoor/outdoor air dry-bulb temperature (DBT) and relative humidity (RH). We evaluated site-specific weather files and compared simulation outputs and measured data using the Root Mean Square Error (RMSE). As a result, the validated model presented 0.56°C to 0.85°C DBT discrepancies and 3.10% to 5.90% RH differences.

Keywords: Uncertainty analysis; Whole-building performance simulation; Survey data; Model Validation.

Resumo

A simulação de desempenho permite interação entre diversos parâmetros físicos, mas representa apenas parte das características do espaço construído. Portanto, processos de calibração podem aumentar sua precisão e melhor representar particularidades do ambiente. Objetivamos calibrar/validar um modelo institucional em Viçosa-MG, testando o método de incertezas paralelo e serial. Conduzimos uma calibração higrotérmica manual/estatística aplicando medições de temperatura (TBS) e umidade (UR). Criamos arquivos climáticos locais e comparamos dados de simulação e medição usando a raiz do Erro Quadrático Médio (EQM). Assim, obtivemos um modelo validado com discrepâncias de 0.56°C à 0.85°C para TBS e 3.10% até 5.90% para UR.

Palavras-chave: Análise de incertezas; Simulação de desempenho para edificação; Medições físicas; Validação.

Como citar:
LUCARELLI, C. D. C.; OLIVEIRA, M. M.; CARLO, J. C. Thermal calibration of an existing institutional building. In: ENCONTRO NACIONAL DE TECNOLOGIA DO AMBIENTE CONSTRUÍDO, 19, 2022, Canela. **Anais**... Porto Alegre: ANTAC, 2022. p. XXX-XXX.

INTRODUCTION

The building modeling and performance simulation (BPS) comprises computer-based representations with physical principles [1]. According to Clarke and Hensen [2], BPS quantifies performance criteria suitable for building design, operation, and control, aiming to portray the dynamicity of physical processes.

However, modeling and simulating the built domain is complicated due to interacting performance expectations and unpredictability. For instance, BPS uncertainties include building geometry, material thermal properties, power consumption of electric and electronic equipment (plug loads), human-generated heat, occupancy schedules, heat gain and loss due to infiltration, and &c. [3]. Therefore, computational models should undergo verification, calibration, and validation procedures [1], as portrayed by different research pieces [4,5].

Hence our goal is to test the parallel and serial calibration procedures using a thermal and energy simulation model. This study combines indoor and outdoor hygrothermal surveys for an institutional building in Viçosa-MG, Brazil (20°45’14’’S and 42°52’54’’W). We evaluate the fittest outdoor data for assembling a simulation weather file that rightly represents surveyed indoor dry-bulb temperatures (DBT) and relative humidity (RH). We also conduct a manual/iterative hygrothermal calibration procedure using uncertainty analysis and statistical techniques for tunning multiple adjacent rooms using Ladybug Tools and sub-packages for Rhino3D+Grasshopper.

THEORETICAL FRAMEWORKS

According to Royapoor and Roskilly [6] and O’Donovan, O’Sullivan, and Murphy [7], BPS only portrays a limited part of a building’s fabric properties, occupants, and weather elements, naturally resulting in inaccuracy. Furthermore, software constraints, scarcity of surveyed input parameters, inaccuracy of weather characterization, incorrect or non-convex model geometries, and distrustful building occupancy and schedules lead to virtual model errors and simulation unpredictability.

Most researchers avoid simulation approaches due to the lack of clarity or confidence in the simulation outputs [3]. Besides, an architect, engineer, constructor, and operator (AECO) will hardly gather reliable building system characteristics.

Hence, BPS should encompass verification, calibration, and validation methods [8]. According to De Wilde [1], the AECO professional scrutinizes the conceptual building description during the verification, evaluating similarities between the actual building and the modeling geometry; the validation process delimits the model’s accuracy and ability to depict real-life spaces, and thus, is the calibration goal.

The calibration consists in revising uncertain modeling parameters to improve congruence between surveyed and simulated data. Calibration is manual/iterative (heuristic), graphical/statistic, or automated [1,7]. Normally, calibration processes adopt data-tunning using default building and operation inputs, modified according to simulation results’ precision.

As an example of a heuristic calibration, O'Donovan, Sullivan, and Murphy [7] validated a whole building energy model using indoor DBT. The authors considered shading, internal loads, and natural ventilation as uncertainties. They applied the Normalized Root Mean Square Error (NRMSE) and Normalized Mean Bias Error (NMBE), achieving 0.8°C to 1.1°C discrepancies with a maximum of 6% NMBE.

METHODOLOGY

According to the Köppen classification, Viçosa-MG is warm and temperate (Cwa) with hot and humid summers and cool to mild winters. The selected building (Fig. 01) is a part of *Universidade Federal de Viçosa Architecture Pós-Graduation Program* (Viçosa-MG 20°45'14''S and 42°52'54''W).

Figure 1: Building thermal and energy model and Ladybug Tools' Honeybee/EnergyPlus zoning.

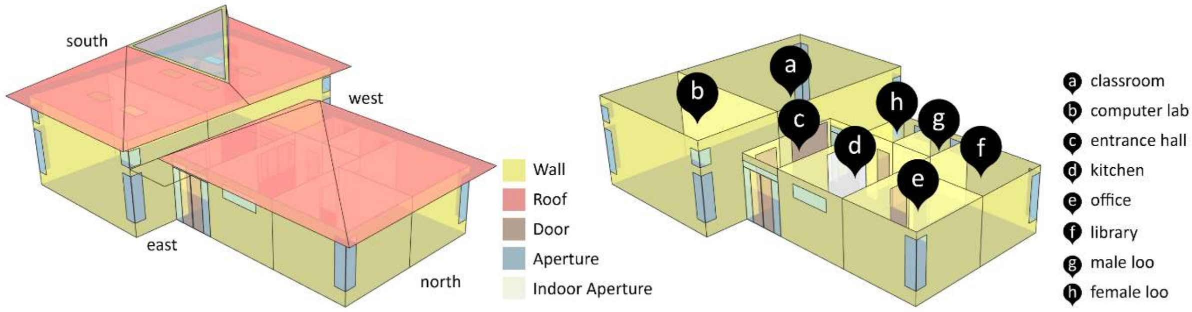

Source: The Authors.

The selected building is 110m^2, one-story, hip/Dutch-like roofed, with eight separate zones. The building is wind-exposed for North and East orientations and displays an expressive microclimate caused by a pond for South and East and a mass of vegetation and surrounding lawn for South and West. The latter represents the building's rear setback, which is also wind-protected.

We divide this study into four methodological procedures according to De Wilde's [1]:

1. Data collection: collecting building components' dimensions; gathering building fabric properties; measuring reflectance values and indoor DBT and RH; surveying occupation and ventilation schedules; estimating plug loads and lighting consumption; establishing uncertainties;
2. Weather data: surveying outdoor DBT and RH for the weather file assemblage; simulating a base case for all created weather files;
3. Simulation and calibration: choosing the fittest weather file created in step two; simulating a new base case; uncertainty analysis and parallel calibration process; serial calibration;
4. Simulation results, evaluation, and validation: comparing surveyed data and simulation results by applying statistical analysis; graphically representing data output using box-plot charts and tables; displaying validated model.

Although De Wilde [1] suggested seven steps, we amalgamate simulation and evaluation and do not adopt re-simulation as a single step since the calibration procedure (item 3) already involves re-simulating the model after each tunning.

FIRST STAGE

We conducted the architectural survey during the first phase, gathering building dimensions (i.e., floorplan, elevations, and aperture sizes). We also examined indoor/outdoor opaque and translucent materials (building fabric), adopting Weber et al.'s [10] equivalent reference models, NBR 15.220-2 and NBR 15.220-3's [11,12] materials and constructions, and NBR NM 294's [13] glass properties.

For instance, Table 1 shows the first base case construction layers, thicknesses (Thk), thermal transmittances (Ut), component thermal capacities (Ct), absorptances (α), solar transmittances (τ), solar reflectance (ρ), emissivity (ε), thermal conductivity (λ), and solar factor (FS). The materials appear from the exterior to the interior, following Ladybug Tools' Honeybee/EnergyPlus construction inputs. We employed an unedited version of TMY3 for Viçosa-MG, which offers the most reliable single-step simulation process with lower computational costs [9].

Table 1: Base case construction and material properties.

<table>
<tr><th colspan="8">Indoor/Outdoor Walls</th></tr>
<tr><td rowspan="6">9-hole brick 9x14x29 cm</td><td>Material</td><td>Thk (cm)</td><td colspan="2">Ut (W/m²°C)</td><td colspan="2">Ct (kJ/m²°C)</td><td>α</td></tr>
<tr><td>Plaster</td><td>2.50</td><td colspan="2" rowspan="5">2.39</td><td colspan="2" rowspan="5">150</td><td>0.2</td></tr>
<tr><td>Ceramic</td><td>1.34</td><td>-</td></tr>
<tr><td>Wall air gap</td><td>6.32</td><td>-</td></tr>
<tr><td>Ceramic</td><td>1.34</td><td>-</td></tr>
<tr><td>Plaster</td><td>2.50</td><td>0.2</td></tr>
<tr><th colspan="8">Roof</th></tr>
<tr><td rowspan="4">Ceramic roof and concrete ceiling</td><td>Material</td><td>Thk (cm)</td><td colspan="2">Ut (W/m²°C)</td><td colspan="2">Ct (kJ/m²°C)</td><td>α</td></tr>
<tr><td>Ceramic Roof Tiles</td><td>1.00</td><td colspan="2" rowspan="3">2.05</td><td colspan="2" rowspan="3">238</td><td>0.75</td></tr>
<tr><td>Air gap</td><td>0.25</td><td>-</td></tr>
<tr><td>Concrete</td><td>10.00</td><td>-</td></tr>
<tr><th colspan="8">Floor</th></tr>
<tr><td rowspan="4">Concrete Slab</td><td>Material</td><td>Thk (cm)</td><td colspan="2">Ut (W/m²°C)</td><td colspan="2">Ct (kJ/m²°C)</td><td>α</td></tr>
<tr><td>Ceramic Tiles</td><td>0.75</td><td colspan="2" rowspan="3">3.59</td><td colspan="2" rowspan="3">2.88</td><td>0.40</td></tr>
<tr><td>Underlayment</td><td>0.50</td><td>-</td></tr>
<tr><td>Concrete</td><td>5.00</td><td>-</td></tr>
<tr><th colspan="8">Windows</th></tr>
<tr><td rowspan="2">Single-Pane Float Glass</td><td>Material</td><td>Thk (cm)</td><td>τ</td><td>ρ</td><td>ε</td><td>λ (W/m.K)</td><td>FS (%)</td></tr>
<tr><td>Glass</td><td>0.3</td><td>0.88</td><td>0.07</td><td>0.84</td><td>1.00</td><td>87.00</td></tr>
</table>

Source: The Authors, adapted from Weber et al. [10], NBR 15.220-2 [11], NBR 15.220-3 [12], NM 294 [13].

We used an ALTA II (eleven wavelengths, from 470 to 940nm) spectrometer to measure surface reflectances, shown in Table 1 as absorptance values (α). We also collected indoor and outdoor DBT and RH from March 9th to March 31st, 2022, using hygrothermal data loggers (HOBO/ONSET U12 Temp/RH/Light accuracy: ±2°C and ±2% RH) recording every five minutes. We used six data loggers indoors (classroom, computer lab, entry hall, kitchen, office, and library) (Fig. 01) and four data loggers outdoors (one for each cardinal orientation).

We surveyed daily occupation patterns, users, electromechanical equipment, and natural conditioning tactics and modeled eight thermal zones (Fig. 01) using Ladybug Tools' Honeybee for Rhino3D+Grasshopper.

Since we monitored the building during the COVID-19 pandemic, there is no occupation on most days. Therefore, we adopted the Ladybug Tools Honeybee Small Office Building Program (Classroom, Lobby, Dining, Closed Office, and Restroom schedules) with default Honeybee office occupation and plug loads on Mondays, Wednesdays, and Fridays from 8 am to 6 pm, compatible with the surveyed occupation data. Other configurations follow Fig. 2 workflow.

Figure 2: Ladybug Tools' Honeybee workflow for occupation/activity schedule and lighting and plug power.

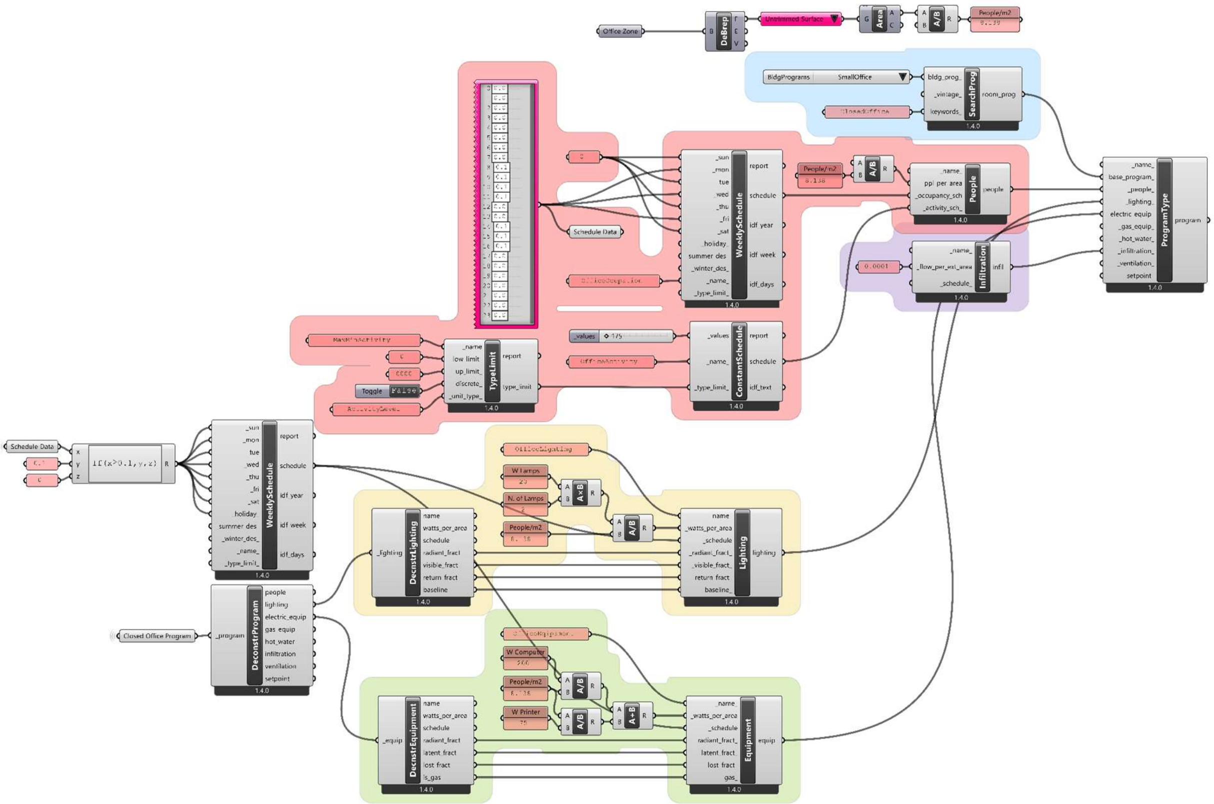

Source: The Authors. Note: Figure in High Resolution for zooming purposes.

We assume construction layers (wall and roof), ventilation (single and cross-flow stances), and soil properties as uncertain input parameters (Table 2). Therefore, we selected two wall constructions from Weber et al. [10] and one from NBR 15.220-3 [12], respecting the surveyed wall thickness and overall visible characteristics. We also selected two ceramic roof structures (i.e., concrete and PVC ceiling) since we could not distinguish all roof layers.

We also evaluated cross and single-flow ventilation. The boundary shading geometry remained as surveyed (i.e., pergola, overhangs, and surrounding vegetation). However, we changed soil aspects by applying dry dust, moist soil, and mud characteristics.

Table 2: Uncertainty Inputs for Building Constructions.

Heat Source	Uncertainty Input			
Walls	**6-hole brick 9x14x24 cm**			
	Material	Thk (cm)	Ut (W/m^2°C)	Ct (kJ/m^2°C)
	Plaster	2.50	2.39	150.00
	Ceramic	1.34		

	Air gap	6.32		
	Ceramic	1.34		
	Plaster	2.50		
	2-hole concrete block 9x19x39cm			
	Material	Thk (cm)	Ut (W/m²°C)	Ct (kJ/m²°C)
	Plaster	2.50	2.79	209.00
	Concrete	1.73		
	Air gap	5.54		
	Concrete	1.73		
	Plaster	2.50		
	Standard brick			
	Material	Thk (cm)	Ut (W/m²°C)	Ct (kJ/m²°C)
	Plaster	2.50	3.13	255.00
	Ceramic	10.00		
	Plaster	2.50		
Roof	**Ceramic roof and concrete slab**			
	Material	Thk (cm)	Ut (W/m²°C)	Ct (kJ/m²°C)
	Ceramic	1.00	2.05	238.00
	Air gap	25.00		
	Concrete	10.00		
	Ceramic roof and PVC ceiling			
	Material	Thk (cm)	Ut (W/m²°C)	Ct (kJ/m²°C)
	Ceramic	1.00	1.75	21.00
	Air gap	25.00		
	PVC ceiling	1.00		
	Underlayment	0.50		
	Concrete	5.00		

Source: The Authors, adapted from Weber et al. [10], NBR 15.220-3 [12].

SECOND STAGE

We collected outdoor DBT and RH using data loggers, protecting the equipment from beam radiation using a 90-degree, 3-way, T-shaped PVC pipe with aluminum foil.

We created five weather files, one for each outdoor-collect data corresponding to each cardinal orientation and one averaging all outdoor DBT and RH data; we edited the TMY3 weather file for Viçosa-MG using the open-source Elements Tool (Big Ladder Software).

We ran simulations for an entire year using the revised files and compared the results with the indoor surveyed data, electing the best-representing file using the Root Mean Square Error (RMSE) and the normalized RMSE (NRMSE) (Equations 1 and 2).

$$RMSE = \sqrt{\frac{\sum_{i=1}^{N}(simulated_i - surveyed_i)^2}{N}} \quad (1)$$

$$NRMSE = \frac{\sqrt{\frac{\sum_{i=1}^{N}(simulated_i - surveyed_i)^2}{N}}}{(max_{simulated} - min_{simulated})} \quad (2)$$

where: *RMSE - Root-Mean-Square Error*
$simulated_i$ - predicted/simulation values
$surveyed_i$ - surveyed data
N - total number of observations
NRMSE – Normalized RMSE
$max_{simulated}$ – maximum simulation value
$min_{simulated}$ – minimum simulation value

THIRD STAGE

After selecting the fittest weather file, we applied two distinct processes for the calibration. The first process comprises a parallel method in which we simulate specific uncertainties for a distinct input parameter (e.g., we simulate 6-hole brick and collect output data; then, we return to the base case and exchange the 6-hole brick with the 2-hole concrete block, and so forth). The second procedure comprises a serial methodology in which we combine all best-rated cases to generate an optimized, validated model.

FOURTH STAGE

We adopted EnergyPlus' Zone DBT and RH outputs and compared the simulation results with indoor surveyed data. We reassessed the methodology adopted in the previous sections, calculating the RMSE and NRMSE.

RESULTS

Table 3 shows RMSE and NRMSE for each assembled weather file simulation data. The results indicate that the TMY3 replaced with South-collected information presents the lowest overall RMSE and NRMSE for DBT and RH. For instance, we utilized NRMSE to compare DBT and RH as it displays results within the same threshold.

Table 3: DBT and RH RMSEs and NRMSEs for each thermal zone using assembled weather files.

RMSEs and NRMSEs for Indoor Air Temperature								
Weather File	**Entry Hall**	**Comp. Lab**	**Classroom**	**Kitchen**	**Library**	**Office**	**RMSE**	**NRMSE**
FileAverage	3.59	3.34	4.23	5.69	5.12	4.90	26.88	1.60
FileNorth	4.26	3.63	4.50	5.74	4.97	4.54	27.64	1.66
FileEast	3.86	3.13	4.00	5.38	4.72	4.33	25.43	1.10
FileSouth	3.03	2.10	2.89	4.55	4.19	3.90	**20.65**	**1.04**
FileWest	3.05	2.10	2.93	4.58	4.20	3.90	20.76	1.39
RMSEs and NRMSEs for Indoor Relative Humidity								
Weather File	**Entry Hall**	**Comp. Lab**	**Classroom**	**Kitchen**	**Library**	**Office**	**RMSE**	**NRMSE**
FileAverage	11.57	11.12	18.05	20.64	19.21	14.40	94.99	1.65
FileNorth	13.37	12.39	18.66	20.28	19.10	14.40	98.20	1.63
FileEast	14.46	13.20	19.75	21.68	20.54	15.52	105.15	1.74
FileSouth	12.14	8.93	13.83	17.61	16.94	13.88	**83.35**	**1.46**
FileWest	12.35	9.45	15.09	18.68	17.90	14.31	87.78	1.53

Source: The Authors.

Furthermore, FileSouth and FileWest delivered comparable results, justified by the proximity of both data loggers to a highly-vegetated, wind-protected boundary condition. We also understand that the collected data for both cardinal orientations is microclimate-affected, reproducing the same conditions in the adjacent rooms.

FileNorth and FileEast are sun and wind-exposed, have higher albedo, and are nearer impermeable surfaces, causing higher dissonances.

Following these results, we appointed FileSouth as the standard substitute for the unedited TMY3 weather file for the new base case simulations. Table 4 depicts each RMSE and NRMSE for the calibration process, displaying constructing materials, ventilation methods, and soil characteristics as separate groups. The parallel calibration process resulted in a pre-selection of the fittest simulation inputs for the future serial calibration. We also present the improvement percentage for each uncertainty compared to the base case.

Table 4: **DBT and RH RMSEs and improvement percentages compared to the base case FileSouth.**

RMSEs for Indoor Air Temperature							
Input Parameter	**Entry Hall**	**Comp. Lab**	**Classroom**	**Kitchen**	**Library**	**Office**	**Improve**
Base Case - FileSouth	3.03	2.10	2.89	4.55	4.19	3.90	-
6-hole brick	0.68	0.79	0.94	2.36	0.67	0.82	69.67%
2-hole concrete block	0.63	0.78	0.89	2.29	0.60	0.89	**70.60%**
Standard brick	0.62	0.86	0.93	2.32	0.64	0.96	69.42%
Ceramic roof and concrete	1.13	1.43	1.98	3.33	1.60	1.43	**47.22%**
Ceramic roof and PVC ceiling	1.51	1.43	2.11	3.75	2.14	1.74	38.69%
Single-flow ventilation	1.03	1.78	1.82	2.71	0.87	1.07	**55.08%**
Cross-ventilation	3.03	2.10	2.89	4.55	5.13	4.01	5.11%
Dry soil	0.89	1.01	1.25	2.63	0.83	1.07	62.79%
Moist Soil	0.89	1.00	1.23	2.62	0.83	1.07	63.03%
Mud	0.88	0.98	1.21	2.61	0.82	1.07	**63.34%**
RMSEs for Relative Humidity							
Input Parameter	**Entry Hall**	**Comp. Lab**	**Classroom**	**Kitchen**	**Library**	**Office**	**Improve**
Base Case – File South	12.14	8.93	13.83	17.61	16.94	13.88	-
6-hole brick	5.53	7.27	9.45	12.85	8.78	7.87	37.91%
2-hole concrete block	5.16	6.67	9.04	12.48	8.11	7.25	**41.54%**
Standard brick	5.00	6.97	9.12	12.59	8.05	7.40	41.05%
Ceramic roof and concrete	7.36	9.17	25.33	18.07	16.07	10.13	3.34%
Ceramic roof and PVC ceiling	5.98	9.03	13.67	16.55	14.11	8.75	**18.32%**
Single-flow ventilation	5.09	9.33	12.58	13.99	9.87	6.51	**31.15%**
Cross-ventilation	12.14	8.93	13.83	17.61	16.94	13.00	1.06%
Dry sand	4.94	6.53	10.17	13.69	9.60	6.51	38.29%
Moist soil	4.93	6.48	10.08	13.65	9.52	6.51	22.60%
Mud	4.93	6.42	9.99	13.60	9.43	6.51	**63.34%**

Source: The Authors.

Even though no wall construction fully represents all surveyed DBT and RH, we understand that we can only choose one for the whole model. Therefore, comparing the improvement rate, we selected the 2-hole concrete block. For the roof construction, the concrete ceiling better represented the model for all rooms, which indicates that, even though we see PVC ceilings in the classroom and computer lab, there is a concrete layer above.

As expected, the single-flow ventilation better represented all cases for DBT. For RH, only the computer lab displayed better RMSEs for cross-ventilation due to its wind-exposed characteristic and the parallel corner windows. Even though the office and library spaces are also wind-exposed, they do not present parallel apertures.

For soil characteristics, mud-like soil showed better RMSEs due to the lawn and vegetation evapotranspiration around all zones.

After defining all suitable simulation inputs, we perform the serial calibration using the 2-hole concrete block, ceramic roof and concrete ceiling, single-flow ventilation, and mud-like soil. For instance, Table 5 demonstrates the lowest overall RMSE among all parallel calibration simulations, the final RMSE outcomes after the serial calibration, and the NRMSE for comparing temperature and humidity outputs.

Table 5: Lowest RMSE for parallel calibration and serial calibration DBT and RH RMSEs and NRMSEs.

	RMSEs and NRMSEs for Indoor Air Temperature						RMSEs and NRMSEs for Relative Humidity					
	Hall	Lab	Class	Kitchen	Library	Office	Hall	Lab	Class	Kitchen	Library	Office
Min. Parallel RMSE	0.60	0.78	0.89	2.17	0.56	0.82	4.93	6.42	9.04	12.07	8.05	6.51
RMSE Serial	0.72	0.67	0.56	0.80	0.85	0.78	5.30	5.90	3.10	5.70	5.60	5.30
NRMSE Serial	0.14	0.14	0.14	0.27	0.27	0.24	0.24	0.20	0.17	0.20	0.23	0.21

Source: The Authors.

Even though RMSEs for RH appear higher than DBT, a comparison of their normalized versions illustrates that the higher deviations occur for DBT in the kitchen, library, and office zones. Overall, we already expected the zones farther from the South to present higher divergences since their boundary conditions differ from the rear setback.

The NRMSE results conform with O'Donovan, Sullivan, and Murphy's [7] results, varying between 0.56°C and 0.85°C and are below 1°C as Rajčić, Skender, and Damjanović [14] recommended. For the RH, the model presented maximum RH divergencies of 5.90%. Rajčić, Skender, and Damjanović [14] indicated that RH between 1% and 10% vary from excellent to acceptable.

Figure 3: Surveyed data, FileSouth base case, and fully-calibrated/validated model.

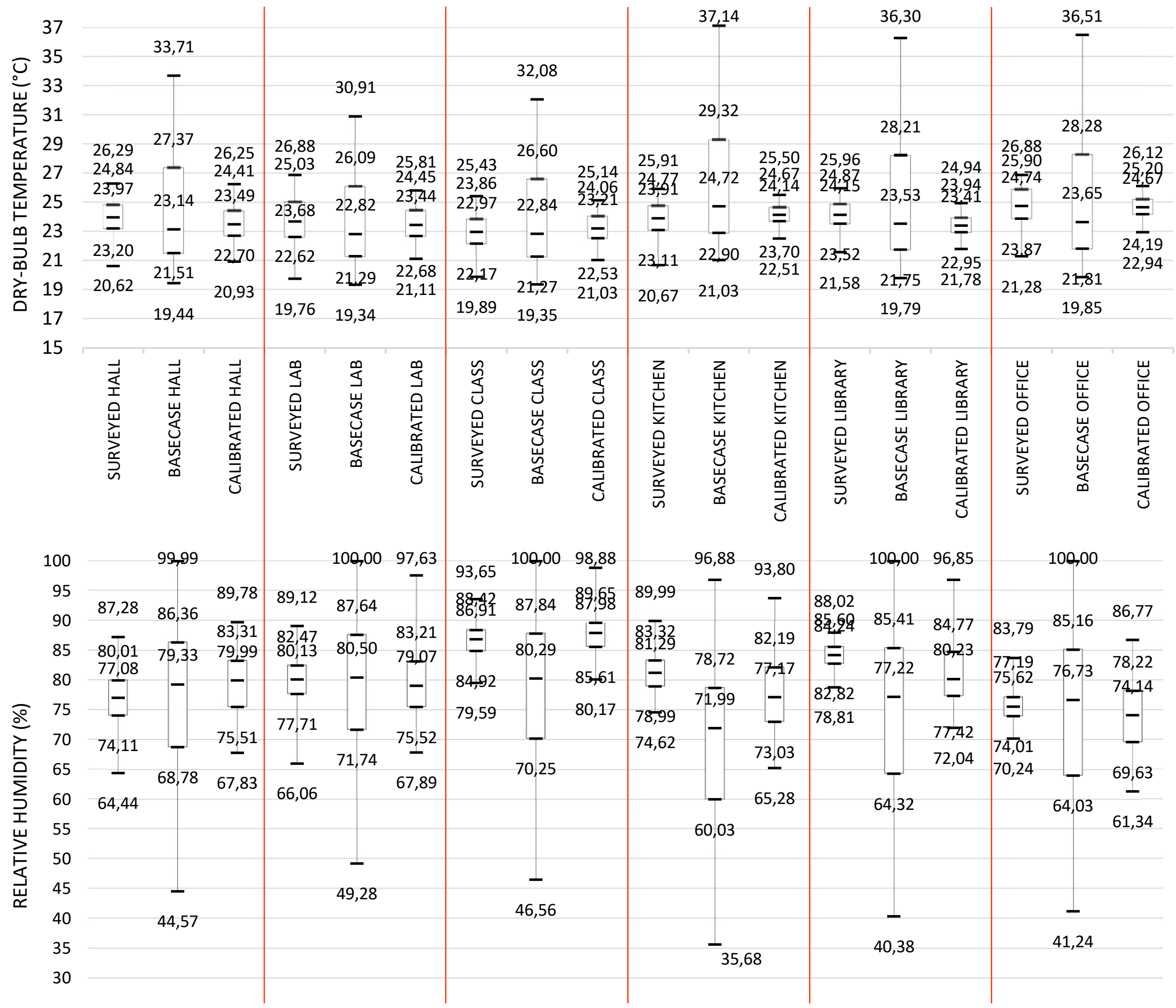

Source: The Authors.

Figure 3 illustrates the calibration/validation process by comparing DBT and RH for surveyed information, FileSouth base case, and the validated model.

CONCLUSIONS

This paper presented a straightforward verification, calibration, and validation procedure for an institutional building in Viçosa-MG applying *in-situ* DBT and RH surveys.

We assembled a fitting weather file based on statistical analysis and utilized parallel and serial uncertainty analysis. Since the building survey occurred during the COVID-19 pandemic, we had a low variability of uncertain inputs due to lacking occupation patterns and plug loads. Also, the Ladybug Tools workflow adopts a simplified version of EnergyPlus' standard simulation procedure, which seldom hinders user override possibilities. However, we found that applying both calibration techniques rendered an optimal model, consistent with the literature, with no further parametric combinations.

Overall, the assembled weather file better-represented rooms adjacent to the data logger placement but did not generate high discrepancies for the other thermal zones. For instance, DBT RMSEs presented 0.56°C to 0.85°C discrepancies, rendering a minimum of 17.58% (library) and a maximum of 31.90% (computer lab) model improvement compared to the FileSouth base case. RH RMSE results were as low as 5.90% for the worst-case scenario, with a maximum improvement of 66.06% (computer lab).

Since our simulation model presents lower divergences than other models using the same calibration/validation procedures [7,14], we consider our model validated.

ACKNOWLEDGEMENTS

This study was financed in part by the Coordenação de Aperfeiçoamento de Pessoal de Nível Superior – Brasil (CAPES) – Finance Code 001 and Fundação de Amparo à Pesquisa de Minas Gerais (FAPEMIG) – Universal Demand 001/2021 Financing Code APQ-00266-21.

REFERENCES

[1] DE WILDE, P. **Building Performance Analysis.** Oxford: John Wiley & Sons Ltd, 2018. DOI: 10.1002/9781119341901.

[2] CLARKE, J.; HENSEN, J. Integrated building performance simulation: Progress, prospects and requirements. **Building and Environment**, v. 91, p. 294–306, 2015. DOI: 10.1016/j.buildenv.2015.04.002.

[3] WESTPHAL, F. **Análise de incertezas e de sensibilidade aplicadas à simulação de desempenho energético de edificações comerciais.** 2007. Tese de Doutorado - Programa de Pós-Graduação em Engenharia Civil, Universidade Federal de Santa Catarina, Florianópolis, 2007.

[4] HUERTO-CARDENAS, H.; LEONFORTE, F.; ASTE, N.; DEL PERO, C.; EVOLA, G.; CONSTANZO, V.; LUCCHI, E. Validation of dynamic hygrothermal Simulation models for historical buildings: State of the art, research challenges and recommendations. **Building and Environment,** v. 180, p. 107081, 2021. DOI: 10.1016/j.buildenv.2020.107081.

[5] MARTÍNEZ-MARINO, S.; EGUÍA-OLLER, P.; GRANADA-ÁLVAREZ, E.; ERKOREKA-GONZÁLEZ, A. Simulation and validation of indoor temperatures and relative humidity in multi-zone

buildings under occupancy conditions using multi-objective calibration. **Building and Environment,** v. 200, 2021. DOI: 10.1016/j.buildenv.2021.107973.

[6] ROYAPOOR, M.; ROSKILLY, T. Building model calibration using energy and environmental data. **Energy and Buildings,** v. 94, p. 109–120, 2015. DOI: 10.1016/j.enbuild.2015.02.050.

[7] O' DONOVAN, A.; O' SULLIVAN, P.; MURPHY, M. Predicting air temperatures in a naturally ventilated nearly zero energy building: Calibration, validation, analysis and approaches. **Applied Energy,** v. 250, p. 991–1010, 2019. DOI: 10.1016/j.apenergy.2019.04.082.

[8] OBERKAMPF, W.; ROY, C. **Verification and Validation in Scientific Computing**. Cambridge: Cambridge University Press, 2010.

[9] GUIMARÃES, Í. B. **Análises de incertezas e sensibilidade de arquivos climáticos e seus impactos em simulações computacionais termo energéticas.** 2016. 95 f. Dissertation (MPhil) - Programa de Pós-Graduação em Arquitetura e Urbanismo, Universidade Federal de Viçosa, Viçosa, 2016.

[10] WEBER, F.; MELO, A.; MANINOSKI, D.; GUTHS, S.; LAMBERTS, R. Desenvolvimento de um modelo equivalente de avaliação de propriedades térmicas para a elaboração de uma biblioteca de componentes construtivos brasileiros para o uso no programa EnergyPlus. 2017. p. 52.

[11] ASSOCIAÇÃO BRASILEIRA DE NORMAS TÉCNICAS. **ABNT NBR 15.220-2:** Desempenho térmico de edificações Parte 2: Métodos de cálculo da transmitância térmica, da capacidade térmica, do atraso térmico e do fator solar de elementos e componentes de edificações. Rio de Janeiro, 2005.

[12] ASSOCIAÇÃO BRASILEIRA DE NORMAS TÉCNICAS. **ABNT NBR 15.220-3:** Zoneamento bioclimático brasileiro e diretrizes construtivas para habitações unifamiliares de interesse social. Rio de Janeiro, 2005.

[13] ASSOCIAÇÃO BRASILEIRA DE NORMAS TÉCNICAS NORMA MERCOSUL. **ABNT NM 294:** Vidro Float. Brasil, Argentina, Uruguai e Paraguai, 2004.

[14] RAJČIĆ, V.; SKENDER, A.; DAMJANOVIĆ, D. An innovative methodology of assessing the climate change impact on cultural heritage. **International Journal of Architectural Heritage**, v. 12, p.21-35, 2018. DOI: 10.1080/15583058.2017.1354094.